ACS NANO

www.acsnano.org

ARTICLE

Graphene-Based Three-Dimensional Capacitive Touch Sensor for Wearable Electronics

Minpyo Kang,[†] Jejung Kim,[†] Bongkyun Jang,[‡] Youngcheol Chae,[†] Jae-Hyun Kim,[‡] and Jong-Hyun Ahn*[,†]

[†]School of Electrical and Electronic Engineering, Yonsei University, Seoul 03722, Republic of Korea

[‡]Department of Applied Nano-Mechanics, Nano Convergence Mechanical Systems Research Division, Korea Institute of Machinery & Materials, Daejeon 34103, Republic of Korea

Supporting Information

ABSTRACT: **The development of input device technology in a conformal and stretchable format is important for the advancement of various wearable electronics. Herein, we report a capacitive touch sensor with good sensing capabilities in both contact and noncontact modes, enabled by the use of graphene and a thin device geometry. This device can be integrated with highly deformable areas of the human body, such as the forearms and palms. This touch sensor detects multiple touch signals in acute recordings and recognizes the distance and shape of the approaching objects before direct contact is made. This technology offers a convenient and immersive human−machine interface and additional potential utility as a multifunctional sensor for emerging wearable electronics and robotics.**

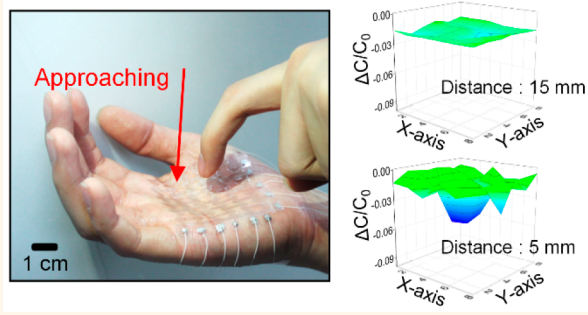

KEYWORDS: *graphene, wearable electronics, stretchable electronics, touch sensor, transparent electrode*

Devices with unusual formats, such as wearable electronics and bendable displays, have advanced rapidly in recent years and serve various functions.[1−6] These devices require wearable or stretchable touch sensors to offer users a convenient input system. The development of flexible, transparent electrode materials is essential for producing touch sensors for wearable or stretchable devices because indium tin oxide (ITO), which is generally used for flat devices, is fragile and rigid[7,8] and poses a challenge for researchers. To address this issue, various transparent electrode materials have been explored for use in wearable touch sensors.[9−14]

Graphene is a promising material for this purpose because it offers numerous benefits, such as mechanical flexibility and optical transmittance.[15−20] There have been several demonstrations of graphene-based touch sensors that show great potential for flexible electronics.[21,22] Flexible, resistive-type touch sensors comprise top and bottom conductive sheets facing each other with a gap between them; these sheets are made of materials such as chemical vapor deposition (CVD)-grown graphene or reduced graphene. However, it is difficult to apply a resistive-type device to wearable applications that need to function in a bent state because the top and bottom electrodes unintentionally make contact with each other, causing a short-circuit during bending, although there are a few reports that resolve this problem.[4,11] Moreover, it is very challenging to detect multipoints of contact with resistive-type devices,[23−25] which restricts their range of applications because many current electronic devices require multitouch sensing that enables users to interact with the system using multiple fingers at once. Currently, capacitive-type touch sensors are considered a good solution for wearable sensing systems with multitouch capability and great sensitivity. It was recently reported that a capacitive touch sensor enabled by CVD-grown graphene[26] provided distinct capabilities in multipoint measurements comparable to those of an ITO-based touch sensor. However, it was designed for flat devices. Aside from capacitive touch-sensing devices, a variety of strain and pressure sensors with good functionality and stretchability based on nanotubes[27] and nanowires[28] have successfully demonstrated feasibility for use in wearable electronic devices. Capacitive-type touch-sensing devices can achieve more effective control of input signals for wearable electronics in highly deformed states, such as stretching or folding. However, although widely known to be

Received: April 10, 2017
Accepted: July 20, 2017
Published: July 20, 2017

DOI: 10.1021/acsnano.7b02474
ACS Nano 2017, 11, 7950−7957

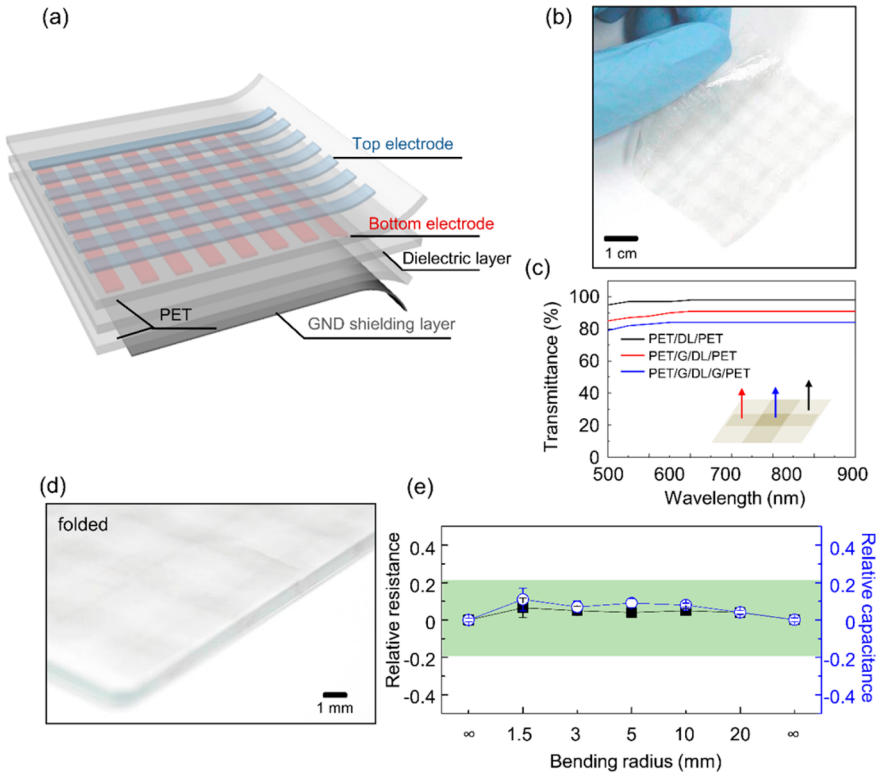

Figure 1. Transparent and flexible graphene-based touch sensor. (a) Schematic diagram illustrating the concept of a graphene-based capacitive sensor. The sensor consists of three layers. The top and bottom layers are composed of patterned graphene electrodes on a PET film substrate. (b) Representative image of an electronic skin with a capacitive, multifunctional sensor array. (c) Optical transmittances for the top and bottom panels of the graphene-based capacitive sensor. (d) Image of a foldable, ultrathin, capacitive sensor that wrapped around the edge of 1 mm-thick glass slide. (e) Relative resistance and capacitance changes under different bending radii.

one of the most promising applications of graphene, the fabrication of stretchable, wearable, and transparent capacitive multitouch sensors remains a challenge. In addition to a position-sensing capability through contact, a three-dimensional (3D)-sensing capability for the recognition of 3D shapes as well as the distance of approaching objects before contact occurs is of increasing interest both in wearable electronic applications and in the robotics field. Although the conventional capacitive 3D sensing has been done with self-capacitance approach to improve the sensitivity, it can suffer from ghost effects requiring additional post processing.[29] Moreover, the number of electrodes is limited (<10 channels), and it has been used only for simple gesture recognition. To address this issue, several approaches based on infrared light,[30] magnetic induction, and ultrasonic waves have been reported, but significant challenges remain in the development of a 3D sensor with high sensitivity, optical transparency, and flexibility that can be fabricated to conform to highly deformable human body parts.

In this study, we present a wearable and stretchable mutual capacitance touch sensor based on graphene electrodes that is capable of multitouch sensing as well as 3D sensing in a highly deformed state. The resulting graphene-based 3D touch sensor can be directly mounted onto deformable human body parts, including the forearms and palms, and it exhibits significant stretchability (~15%) and good sensing capability in contact as well as noncontact modes (22 dB SNR at 7 cm distance).

RESULTS AND DISCUSSTION

Parts a and b of Figure 1 present an optical microscopy image and a schematic of a graphene-based touch sensor with an overall area of 4 × 6 cm^2 and 8 × 8 array (64 channels). The device comprises four main components: (i) a top and bottom made of ultrathin polyethylene terephthalate (PET, thickness ~5 μm); (ii) top and bottom transparent electrode arrays based on triple-layer graphene which was chemically doped with bis(trifluoromethane) sulfonamide (TFSA) (conductivity ~317.1 ohm/sq); (iii) a dielectric layer (acrylic polymer, thickness ~25 μm) for insulating the two electrodes; and (iv) a graphene monolayer at the bottom for grounding. This bottom layer eliminates electrical noise caused by the surface charge on human skin and prevents sweat from penetrating into the active device layers. The width of the patterned graphene electrode and the space between the electrodes are 3 and 4 mm, respectively. The spaces between the graphene electrodes are designed to maximize the sensitivity of the capacitive touch sensor.[31] The worst optical transmittance is 84.6% and occurs when the top and bottom graphene lines overlap (Figure 1c). The good mechanical properties of graphene and the thin geometry of the device enable conformal contact on curved surfaces, *e.g.*, parts of the human body. Solid mechanical modeling of the device layout based on the elastic modulus of the material of each layer indicates that the maximum strain in each layer is less than 1.1% at a bending radius of 1.5 mm (Supporting Information, Figure S1). According to such a small internal strain, when wrapped over the edge of glass slide with a thickness of 1.5 mm, the device displayed a negligible difference in its electrical properties before and after bending (Figure 1d).

DOI: 10.1021/acsnano.7b02474
ACS Nano 2017, 11, 7950−7957

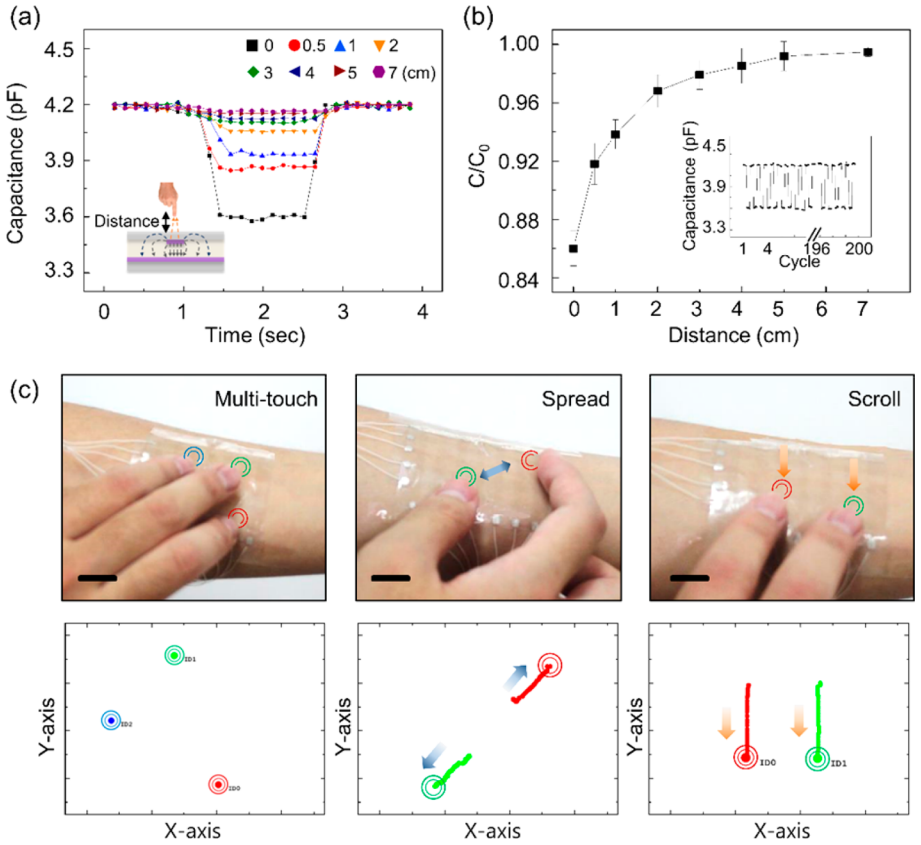

Figure 2. Electrical properties and performances of touch sensor. (a) Capacitance change *versus* time for finger touch and proximity of various distances between 0 and 7 cm. (b) Relative capacitance change ($\Delta C/C_0$) versus distance between sensor and finger. The inset shows the test repeated for 200 cycles. (c) Image of wearable capacitive touch sensor fabricated using graphene electrodes. The images below show the touch sensor monitor and the multitouch, spread, and scroll performances. Scale bar, 2 cm.

Figure 1e presents the changes in both the capacitances of the device substrates and the line resistances of the graphene electrodes measured at different bending radii, which are both within 0.2. As a result, the maximum variations of the time constants are only 4%, which guarantees a reliable scanning time, even after bending. The resistance of the graphene electrodes and the capacitance of the dielectric layer remain virtually unperturbed even at a bending radius of 1.5 mm; moreover, they perfectly recovered after returning to an unbent state. The touch sensor can provide information about touch points by measuring changes in mutual capacitance between the top and bottom electrodes.

Parts a and b of Figure 2 show the change in the mutual capacitance and the ratio between this change and the unperturbed value for different distances between the fingers and the touch sensor, respectively. The bottom electrode is driven to provide an electric field with a sequential driving method. When a finger approaches the surface of the sensor, part of the fringing electric field is absorbed (Supporting Information, Figure S2). This local reduction can be measured individually in each cross point (inset of Figure 2a).[32,33] When a finger touches the sensor, a capacitance change (ΔC) of 0.61 pF is measured with a 4.19 pF baseline capacitance, resulting in a 14.5% change in the mutual capacitance. The response time of this device is about 60 ms, which is comparable with reported values[28,34−36] (Supporting Information, Figure S3 and Table S1). Contactless touch for the perception of the distance and 3D shape of an approaching object is also measured, and Figure 2b shows the detected finger distance as the height of the finger above the touch sensor is varied. At a range of 0.5 cm, the SNR of 32 dB and the ΔC of 0.34 pF are sensed with a standard deviation of 15 fF, and a finger can be clearly detected up to a maximum range of 7 cm with the measured ΔC of 50 fF and SNR of 22 dB. Moreover, the initial capacitance value recovers completely after removing the finger and exhibits good reliability even after 200 test cycles (inset of Figure 2b and Supporting Information, Figure S4).

A capacitive touch sensor with good sensibility and reliability, structured as an 8 × 8 channel array, was mounted to a user's forearm for touch-sensing experiments. The ability of an input device to be mounted onto and conform to the human body is important for improving the convenience of wearable electronics. An interface board with an offset-calibration, which compensated for parasitic capacitance from the lead wires and the surrounding environment, was connected to the touch sensor *via* flexible interconnecting wires, which evaluated the touch points and transferred data to the display. In addition, the device was operated with low power consumption because it was based on circuits developed for conventional ITO-based ones. To stably operate a touch sensor on the skin, it was necessary to preclude any influence from the surface of the skin. Thus, a graphene monolayer was laminated onto the back side of the PET substrate for ground shielding. The graphene layer acting as a ground shield effectively reduced skin noise and the effect of sweat, resulting in a decrease in SNR value (Supporting Information, Figures S5 and S6). In addition, the hydrophobicity of the graphene sheet effectively blocked the penetration of sweat created from the skin. The devices had

DOI: 10.1021/acsnano.7b02474
ACS Nano 2017, 11, 7950−7957

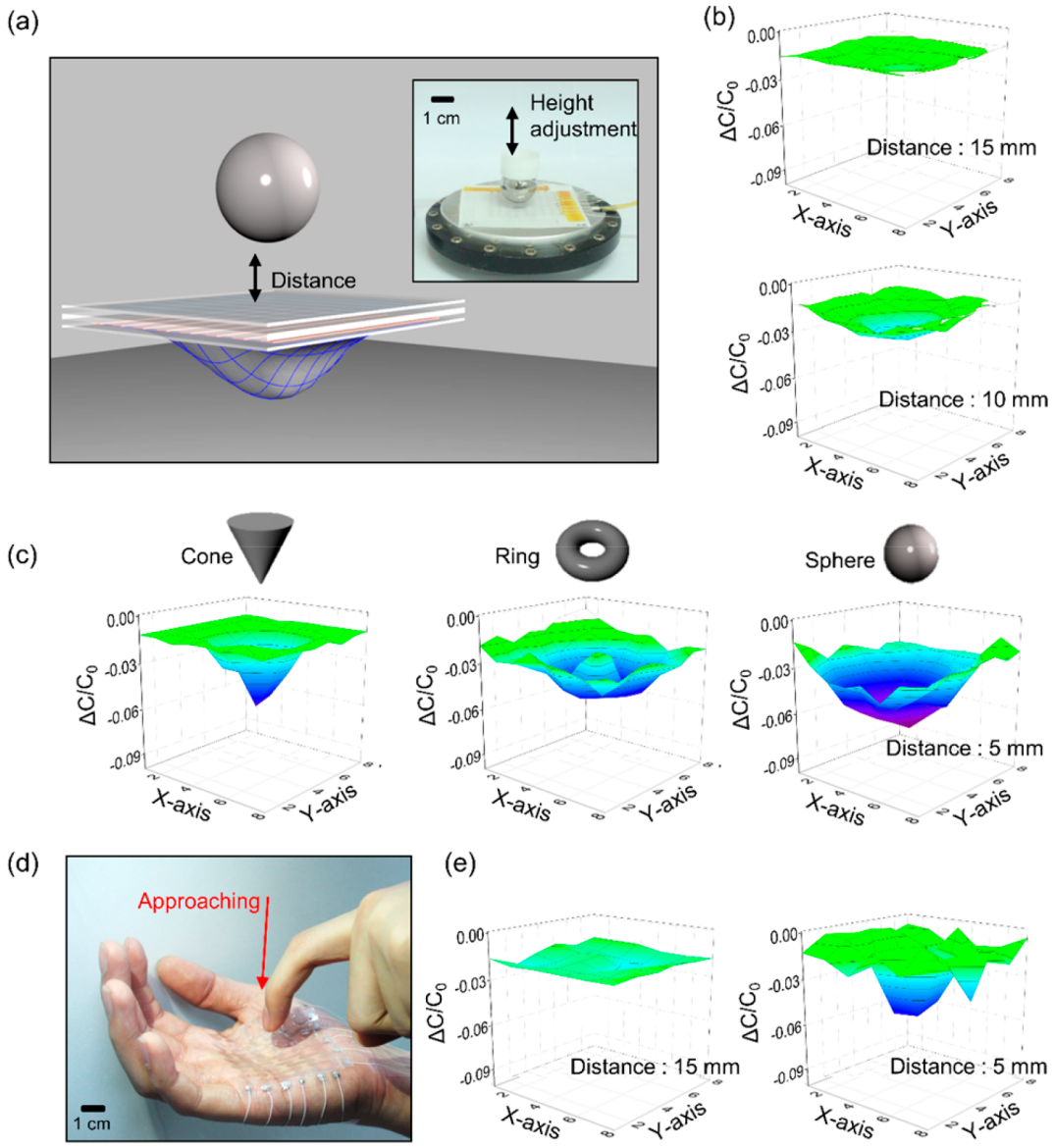

Figure 3. 3D measurement of approaching objects. (a) Schematic illustration of 3D measurements in noncontact mode. A conductive iron sphere was used for measurements. The inset shows a view of the measurement setup. (b) 3D mapping graph of relative capacitive changes over three different distances between the object and sensor (15, 10, and 5 mm). The plotted surfaces indicate the mapping results of relative capacitance changes from the 8 × 8 capacitive sensor array. (c) Detection of various shapes such as cone (left), ring (middle), and sphere (right). All objectives are 5 mm apart from the center of the sensor. (d) Optical image of 3D sensor on the palm with approaching finger. (e) Capacitance change for approaching finger by 15 and 5 mm.

three representative operation modes, *i.e.*, multitouch, spread, and scroll, which are commonly used for conventional smartphones, and all of these modes were exhibited even on a curved forearm, which has not been achieved by resistive-type touch sensors or typical strain sensors (Figure 2c and Supporting Information, movie S1).[37] This sensor cannot directly measure the pressure applied by objects because it is based on measuring the change in capacitance of dielectrics between two electrodes, in contrast to electronic skins which show a good pressure sensing properties in low-pressure regimes of <10 kPa.[4,35] The capacitance of the touch sensors mounted on the skin was affected by changes in body temperature because the dielectric constant of the insulating layer increased under thermal heating, resulting in an increase in capacitance.[38] The baseline capacitance of the touch sensors increased slightly from 4.19 to 4.24 pF after being mounted onto the forearm (*i.e.*, after the temperature increased from room temperature, 25 °C, to body temperature, 36.5 °C). Such a steady baseline increase did not cause problems with the sensing capability. In contrast, an irregular change in body temperature could have a negative effect on the sensing capability. A slight capacitance change of 0.029 pF ± 1.8% was observed in response to a temperature change from 35 to 40 °C. In addition, we examined the effect of humidity on the touch sensor because it can irregularly change the capacitance of touch sensor. As humidity increased from 30% to 60%, the touch sensor showed a slight change by less than 2.5% (Supporting Information, Figure S7).[34,39] Such baseline or temperature-induced changes can be easily compensated for *via* foreground calibration, with which interface boards are typically equipped.

DOI: 10.1021/acsnano.7b02474
ACS Nano 2017, 11, 7950–7957

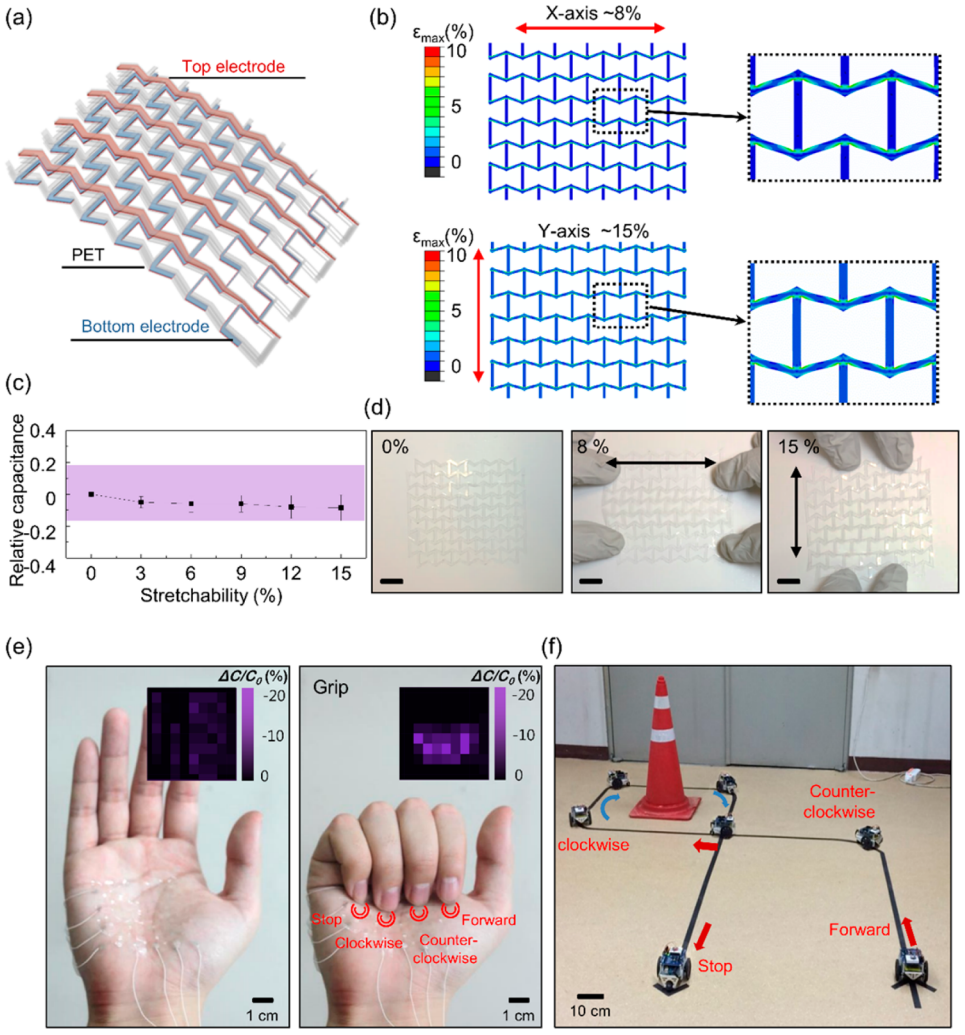

Figure 4. Stretchable auxetic touch sensor. (a) Schematic illustration of mesh-type structure capacitive sensor. Red and blue colors indicate top and bottom electrodes, respectively. (b) FEM strain distribution analysis for strain distribution along *X*-axis (top) and *Y*-axis (bottom). (c) Relative resistance and capacitance changes under different tensile strains. (d) Images of graphene capacitive sensor stretched under different applied strains: undeformed status (left), 8% stretched in *X*-axis (middle), and 15% stretched status in *Y*-axis (right). Scale bar, 1 cm. (e) Optical images of stretchable devices mounted on palm for remote controlling the toy car. Inset of each image shows relative capacitance changes for spread (left) and grip (right) status of the hand. (f) Images of car controlled by capacitive sensor signals on palm.

3D sensors are important devices for various wearable electronic applications, *e.g.*, electronic skin for robots, and require the ability to accurately detect objects without contact. In contrast to previous approaches,[40,41] our graphene-based capacitive touch device enables the detection of 3D shapes and the location of nearby conductive objects when integrated with highly deformable human body parts. Figure 3a shows the proximity measurements of 3D conductive objects shaped as a sphere, cone, or doughnut. When a 2 cm diameter iron sphere approached the touch sensor, the capacitance gradually decreased to −2.5, −3.2, and −6.7% as the space between the sphere and sensor decreased from 15 to 5 mm (Figure 3b,c, right). In addition to the distance, different object shapes induce different changes in capacitance, enabling the recognition of different object forms. As the sphere nears the sensor, its hemispherical, 3D shape is more clearly recognized by the mapping data. When it moves in the *X*−*Y* plane, this is obviously observed by changes in the mapping images (Supporting Information, Figure S8). These results indicate that the sensor is capable of detecting shape and movement in three axes. To characterize the spatial resolution of the sensor in noncontact mode, three different objects were measured, a metal cone, a metal ring, and a sphere (Figure 3c and Supporting Information, Figure S9). The cone has a vertex that induces a prominent disturbance in the electric field, resulting in a deep, valley-like mapping image, which can be recognized as a cone in contrast with a sphere. The metal ring resulted in a mapping image that clearly shows the inner empty space of the ring. In addition to conductive metal objects, the touch sensor with the structural design in a stretchable format on palm clearly detects the movement of an approaching finger (Figure 3d,e, Supporting Information, Figure S10). Although this device is based on mutual capacitance touch sensor which enables clear sensing of multitouch points without ghost positions, it achieved comparable sensitivity with the state-of-the art capacitive touch sensor[29] which relies on self-capacitance type. It shows a significant improvement in sensitivity, considering that the sensitivity of self-capacitance sensor is generally 1 order of magnitude higher than that of mutual type under the same set of conditions. Thus, this device enables us to fabricate large area applications including robotics and 3D gesture sensing system.

DOI: 10.1021/acsnano.7b02474
ACS Nano 2017, 11, 7950−7957

Adding mechanical stretchability to a touch sensor can extend its range of wearable electronic applications. The stretchability of the device improved by 8−15% in the X and Y directions by introducing an auxetic mesh structure (Figure 4a). The dielectric layer was added between two graphene electrode lines (blue on the bottom and red on the top) to form a capacitive touch sensor (Supporting Information, Figure S11). The perforated auxetic structure[42,43] could effectively transform the applied tensile strain into local bending motions of the constituent beams, resulting in an improved stretchability of the touch device. Furthermore, the perforated auxetic structure could simultaneously induce stretching in both the X and Y directions upon tensile loading, in contrast to other structures such as honeycomb structures,[44,45] which result in shrinkage in the X direction in response to stretching in the Y direction. As a result, a perforated auxetic structure can improve the stability of touch sensors attached to human body parts, such as palms, which expand biaxially. Strain distributions under applied tensile strains were evaluated using finite element analysis (FEA) with a representative volume-element model (Figure 4b). Figure 4b shows the maximum principal strain distribution when uniaxial strain was applied in the X (top) and the Y (bottom) directions. The simulation results show that this structure is stretchable by up to 8% in the X direction and up to 15% in the Y direction without device failure, and these results agree well with the experimental results shown in Figure 4d. Relative capacitance decreased slightly to 5% at the maximum tensile strain along the X and Y axes because the interference between adjacent electrodes was reduced by stretching (Figure 4c). Such a change in capacitance by strain could disturb clear touch sensing. When a strain sensor was integrated with this device, it could calibrate the effect of strain on the capacitance. The thinness and mechanical stretchability of the entire device, including the graphene electrodes, insulators, and substrates, could create conformal contact with highly deformable human body parts. For example, the stretchable touch device was mounted and strongly attached along the lines of the palm (Figure 4e). The device can also be used for various other applications, such as remote controllers or assistive communication devices. For example, a varied sequence of contacts with different numbers of fingers can produce a sequence of electrical signals that can be converted into a command to control an automobile. A simple finger motion can control the movement of a toy car (Figure 4f and Supporting Information, movie S2). This device comprises four buttons for controlling different actions, including moving forward, rotating clockwise, rotating counterclockwise, and stopping.

CONCLUSION

While a considerable amount of research has been conducted on the development of graphene-based touch sensors for a variety of practical applications over the past decade, many limitations remain. Only touch sensors designed for rigid electronics and resistive-type touch sensors for detecting a single touch have been demonstrated because of the difficulty involved in fabricating capacitive, 3D, multitouch sensors based on transparent graphene electrodes in a wearable or stretchable format. The wearable and stretchable capacitive touch sensor presented here addresses these difficulties by enabling multi-finger touch sensing as well as 3D sensing while mounted on highly deformable human body parts. The use of graphene as a transparent electrode enables the fabrication of a thin and stretchable device, which improves the resulting functionality and capabilities by minimizing mechanical failure during operation. Although much effort will be required to render the approach presented here compatible with currently existing technology and applicable to practical devices, this is a potential route toward a key application of graphene in emerging wearable electronics.

METHODS

Graphene Synthesis and Fabrication of Devices. Graphene was grown by chemical vapor deposition on a Cu foil, and Cu was subsequently etched in ammonium persulfate (20 g dissolved in 1000 mL of deionized water) after coating poly(methyl methacrylate) as a supporting layer. Then the graphene was transferred onto a PET substrate. The transferred graphene was patterned using photolithography and oxygen plasma etching. TFSA was used for chemical doping of triple-layer graphene, which showed the improvement of ∼30% in electrical conductivity (Supporting Information, Figure S12). After the entire process of device fabrication, the device was mounted on skin using thin adhesive (Liquid bandage; 3 M Nexcare, thickness: ∼200 nm) for stable operation.[46]

Finite Element Analysis. FEA on mesh-type devices (Figure 3c) was conducted using a commercial code, ABAQUS. A quadratic quadrilateral element for plane stress was adopted with reduced integration, and the number of elements was set to 17052. We numerically analyzed a single representative volume element (RVE) with periodic boundary conditions and a nonlinear deformation option under uniaxial tensile strain along the x or y directions. The Young's modulus (E) and Poisson ratio (ν) of the materials are indicated in Table S2.

Measurements of Finger Touch and 3-D Touch. Capacitance measurements of the graphene-based capacitive sensor were acquired using a Keithley 590 CV analyzer (Keithley Instruments, Inc.). Capacitance was established using a two-electrode configuration at 500 kHz with 3.3 V of supplying voltage. The change in capacitance was measured by applying a finger or touch pen repeatedly. It was also confirmed that the capacitance completely recovered its initial value after releasing the contact. Other conditions, including temperature and humidity, were strictly controlled to obtain a precise measurement.

ASSOCIATED CONTENT

Supporting Information

The Supporting Information is available free of charge on the ACS Publications website at DOI: 10.1021/acsnano.7b02474.

Strain values of each layer in various bending radius, mechanisms of touch and proximity sensor detection, stability test for 200 cycles, ground-shielding effect of touch panel, 3D tracking of the conductive iron sphere, 3D modeling measurement system, device structure of mesh type capacitive sensor, and mechanical properties and thickness of constituent materials of 3D touch sensor (PDF)

Movie S1 (AVI)

Movie S2 (AVI)

AUTHOR INFORMATION

Corresponding Author

*E-mail: ahnj@yonsei.ac.kr.

ORCID

Bongkyun Jang: 0000-0002-8247-7229

Jong-Hyun Ahn: 0000-0002-8135-7719

Notes

The authors declare no competing financial interest.

DOI: 10.1021/acsnano.7b02474
ACS Nano 2017, 11, 7950−7957

ACKNOWLEDGMENTS

This work was supported by the National Creative Research Laboratory (2015R1A3A2066337) through the National Research Foundation of Korea (NRF).

REFERENCES

(1) Kim, D.-H.; Lu, N.; Ma, R.; Kim, Y.-S.; Kim, R.-H.; Wang, S.; Wu, J.; Won, S. M.; Tao, H.; Islam, A.; Yu, K. J.; Kim, T.-I.; Chowdhury, R.; Ying, M.; Xu, L.; Li, M.; Chung, H.-J.; Keum, H.; McCormick, M.; Liu, P.; Zhang, Y.-W.; Omenetto, F. G.; Huang, Y.; Coleman, T.; Rogers, J. A. Epidermal Electronics. *Science* **2011**, *333*, 838−843.

(2) Kim, J.; Lee, M.; Shim, H.-J.; Ghaffari, R.; Cho, H.-R.; Son, D.; Jung, Y.-H.; Soh, M.; Choi, C.; Jung, S.; Chu, K.; Jeon, D.; Lee, S.-T.; Kim, J.-H.; Choi, S.-H.; Hyeon, T.; Kim, D.-H. Stretchable Silicon Nanoribbon Electronics for Skin Prosthesis. *Nat. Commun.* **2014**, *5*, 5747.

(3) Lee, M.-S.; Lee, K.; Kim, S.-Y.; Lee, H.; Park, J.; Choi, K.-H.; Kim, H.-K.; Kim, D.-G.; Lee, D.-Y.; Nam, S.; Park, J.-U. High-performance, Transparent, and Stretchable Electrodes Using Graphene−Metal Nanowire Hybrid Structures. *Nano Lett.* **2013**, *13*, 2814−2821.

(4) Lee, S.; Reuveny, A.; Reeder, J.; Lee, S.; Jin, H.; Liu, Q.; Yokota, T.; Sekitani, T.; Isoyama, T.; Abe, Y.; Suo, Z.; Someya, T. A Transparent Bending-Insensitive Pressure Sensor. *Nat. Nanotechnol.* **2016**, *11*, 472−478.

(5) Ho, D. H.; Sun, Q.; Kim, S. Y.; Han, J. T.; Kim, D. H.; Cho, J. Stretchable and Multimodal All Graphene Electronic Skin. *Adv. Mater.* **2016**, *28*, 2601.

(6) Kaltenbrunner, M.; Sekitani, T.; Reeder, J.; Yokota, T.; Kuribara, K.; Tokuhara, T.; Drack, M.; Schwödiauer, R.; Graz, I.; Bauer-Gogonea, S.; Bauer, S.; Someya, T. An Ultra-Lightweight Design for Imperceptible Plastic Electronics. *Nature* **2013**, *499*, 458−463.

(7) Tuna, O.; Selamet, Y.; Aygun, G.; Ozyuzer, L. High Quality ITO Thin Films Grown by DC and RF Sputtering without Oxygen. *J. Phys. D: Appl. Phys.* **2010**, *43*, 055402.

(8) Leterrier, Y.; Médico, L.; Demarco, F.; Månson, J.-A. E.; Betz, U.; Escolà, M. F.; Kharrazi Olsson, M.; Atamny, F. Mechanical Integrity of Transparent Conductive Oxide Films for Flexible Polymer-Based Displays. *Thin Solid Films* **2004**, *460*, 156−166.

(9) Im, H.-G.; Jin, J.; Ko, J.-H.; Lee, J.; Lee, J.-Y.; Bae, B.-S. Flexible Transparent Conducting Composite Films Using a Monolithically Embedded AgNW Electrode with Robust Performance Stability. *Nanoscale* **2014**, *6*, 711−715.

(10) Im, H.-G.; Jung, S.-H.; Jin, J.; Lee, D.; Lee, J.; Lee, D.; Lee, J.-Y.; Kim, I.-D.; Bae, B.-S. Flexible Transparent Conducting Hybrid Film Using a Surface-Embedded Copper Nanowire Network: A Highly Oxidation-Resistant Copper Nanowire Electrode for Flexible Optoelectronics. *ACS Nano* **2014**, *8*, 10973−10979.

(11) Wu, H.; Kong, D.; Ruan, Z.; Hsu, P.; Wang, S.; Yu, Z.; Carney, T. J.; Hu, L.; Fan, S.; Cui, Y. A Transparent Electrode Based on a Metal Nanotrough Network. *Nat. Nanotechnol.* **2013**, *8*, 421−425.

(12) Lee, J.-Y.; Connor, S. T.; Cui, Y.; Peumans, P. Solution-Processed Metal Nanowire Mesh Transparent Electrodes. *Nano Lett.* **2008**, *8*, 689−692.

(13) Cai, G.; Darmawan, P.; Cui, M.; Wang, J.; Chen, J.; Magdassi, S.; Lee, P. S. Highly Stable Transparent Conductive Silver Grid/PEDOT:PSS Electrodes for Integrated Bifunctional Flexible Electrochromic Supercapacitors. Adv. *Energy Mater.* **2016**, *6*, 1501882.

(14) Kim, C.-C.; Lee, H.-H.; Oh, K.; Sun, J.-Y. Highly Stretchable, Transparent Ionic Touch Panel. *Science* **2016**, *353*, 682−687.

(15) Hecht, D. S.; Hu, L.; Irvin, G. Emerging Transparent Electrodes Based on Thin Films of Carbon Nanotubes, Graphene, and Metallic Nanostructures. *Adv. Mater.* **2011**, *23*, 1482−1513.

(16) Jang, H.; Park, Y. J.; Chen, X.; Das, T.; Kim, M.-S.; Ahn, J.-H. Graphene-Based Flexible and Stretchable Electronics. *Adv. Mater.* **2016**, *28*, 4184−4202.

(17) Park, J.-U.; Nam, S.; Lee, M.-S.; Lieber, C. M. Synthesis of Monolithic Graphene−Graphite Integrated Electronics. *Nat. Mater.* **2012**, *11*, 120−125.

(18) Bonaccorso, F.; Sun, Z.; Hasan, T.; Ferrari, A. C. Graphene Photonics and Optoelectronics. *Nat. Photonics* **2010**, *4*, 611−622.

(19) Kim, K.; Bae, S.-H.; Toh, C. T.; Kim, H.; Cho, J. H.; Whang, D.; Lee, T.-W.; Özyilmaz, B.; Ahn, J.-H. Ultrathin Organic Solar Cells with Graphene Doped by Ferroelectric Polarization. *ACS Appl. Mater. Interfaces* **2014**, *6*, 3299−3304.

(20) Hyun, W. J.; Secor, E. B.; Hersam, M. C.; Frisbie, C. D.; Francis, L. F. High-Resolution Patterning of Graphene by Screen Printing with a Silicon Stencil for Highly Flexible Printed Electronics. *Adv. Mater.* **2015**, *27*, 109−115.

(21) Bae, S.; Kim, H.; Lee, Y.; Xu, X.; Park, J.-S.; Zheng, Y.; Balakrishnan, J.; Lei, T.; Kim, H. R.; Song, Y. I.; Kim, Y.-J.; Kim, K. S.; Özyilmaz, B.; Ahn, J.-H.; Hong, B. H.; Iijima, S. Roll-to-Roll Production of 30-in. Graphene Films for Transparent Electrodes. *Nat. Nanotechnol.* **2010**, *5*, 574.

(22) Wang, J.; Liang, M.; Fang, Y.; Qiu, T.; Zhang, J.; Zhi, L. Rod-Coating: Towards Large-Area Fabrication of Uniform Reduced Graphene Oxide Films for Flexible Touch Screens. *Adv. Mater.* **2012**, *24*, 2874−2878.

(23) Lee, J.; Lee, P.; Lee, H. B.; Hong, S.; Lee, I.; Yeo, J.; Lee, S. S.; Kim, T.-S.; Lee, D.; Ko, S. H. Room-Temperature Nanosoldering of a Very Long Metal Nanowire Network by Conducting-Polymer-Assisted Joining for a Flexible Touch-Panel Application. *Adv. Funct. Mater.* **2013**, *23*, 4171−4176.

(24) Im, H.-G.; An, B. W.; Jin, J.; Jang, J.; Park, Y.-G.; Park, J.-U.; Bae, B.-S. A high-performance, flexible and robust metal nanotrough-embedded transparent conducting film for wearable touch screen panels. *Nanoscale* **2016**, *8*, 3916−3922.

(25) Hecht, D. S.; Thomas, D.; Hu, L.; Ladous, C.; Lam, T.; Park, Y.; Irvin, G.; Drzaic, P. Carbon-Nanotube Film on Plastic as Transparent Electrode for Resistive Touch Screens. *J. Soc. Inf. Disp.* **2009**, *17*, 941.

(26) Ryu, J.; Kim, Y.; Won, D.; Kim, N.; Park, J. S.; Lee, E.-K.; Cho, D.; Cho, S.-P.; Kim, S. J.; Ryu, G. H.; Shin, H. S.; Lee, Z.; Hong, B. H.; Cho, S. Fast Synthesis of High-Performance Graphene Films by Hydrogen-Free Rapid Thermal Chemical Vapor Deposition. *ACS Nano* **2014**, *8*, 950−956.

(27) Lipomi, D. J.; Vosgueritchian, M.; Tee, B. C.-K.; Hellstrom, S. L.; Lee, J. A.; Fox, C. H.; Bao, Z. Skin-like Pressure and Strain Sensors Based on Transparent Elastic Films of Carbon Nanotubes. *Nat. Nanotechnol.* **2011**, *6*, 788−792.

(28) Yao, S.; Zhu, Y. Wearable Multifunctional Sensors Using Printed Stretchable Conductors Made of Silver Nanowires. *Nanoscale* **2014**, *6*, 2345−2352.

(29) Hu, Y.; Huang, L.; Rieutort-Louis, W.; Sanz-Robinson, J.; Wagner, S.; Sturm, J. C.; Verma, N. 3D Gesture-Sensing System for Interactive Displays Based on Extended-Range Capacitive Sensing. *IEEE Int. Solid-State Circuits Conf. Dig. Technol. Papers* **2014**, 212−213.

(30) Chen, E.-C.; Shih, C.-Y.; Dai, M.-Z.; Yeh, H.-C.; Chao, Y.-C.; Meng, H.-F.; Zan, H.-W.; Liu, W.-R.; Chiu, Y.-C.; Yeh, Y.-T.; Sun, C.-J.; Horng, S.-F.; Hsu, C.-S. Polymer Infrared Proximity Sensor Array. *IEEE Trans. Electron Devices* **2011**, *58*, 1215−1220.

(31) Gao, S.; Lai, J.; Micou, C.; Nathan, A. Reduction of Common Mode Noise and Global Multivalued Offset in Touch Screen Systems by Correlated Double Sampling. *J. Disp. Technol.* **2016**, *12*, 639−645.

(32) Zhang, B.; Xiang, Z.; Zhu, S.; Hu, Q.; Cao, Y.; Zhong, J.; Zhong, Q.; Wang, B.; Fang, Y.; Hu, B.; Zhou, J.; Wang, Z. Dual functional transparent film for proximity and pressure sensing. *Nano Res.* **2014**, *7*, 1488−1496.

(33) Cotton, D. P. J.; Graz, I. M.; Lacour, S. P. A Multifunctional Capacitive Sensor for Stretchable Electronic Skins. *IEEE Sens. J.* **2009**, *9*, 2008−2009.

(34) Kim, S.; Park, S.; Park, H.; Park, D.; Jeong, Y.; Kim, D. Highly Sensitive and Multimodal All-Carbon Skin Sensors Capable of Simultaneously Detecting Tactile and Biological Stimuli. *Adv. Mater.* **2015**, *27*, 4178−4185.

DOI: 10.1021/acsnano.7b02474
ACS Nano 2017, 11, 7950−7957

(35) Mannsfeld, S. C. B; Tee, B. C. K; Stoltenberg, R. M.; Chen, C. V. H. H; Barman, S.; Muir, B. V. O; Sokolov, A. N.; Reese, C.; Bao, Z. Highly Sensitive Flexible Pressure Sensors with Microstructured Rubber Dielectric Layers. *Nat. Mater.* **2010**, *9*, 859−864.
(36) Lee, J.; Kwon, H.; Seo, J.; Shin, S.; Koo, J. H.; Pang, C.; Son, S.; Kim, J. H.; Jang, Y. H.; Kim, D. E.; Lee, T. Conductive Fiber-Based Ultrasensitive Textile Pressure Sensor for Wearable Electronics. *Adv. Mater.* **2015**, *27*, 2433−2439.
(37) Park, M.; Park, Y. J.; Chen, X.; Park, Y.-K.; Kim, M.-S.; Ahn, J.-H. MoS_2-Based Tactile Sensor for Electronic Skin Applications. *Adv. Mater.* **2016**, *28*, 2556−2562.
(38) Matsuguchi, M.; Sadaoka, Y.; Sakai, Y.; Kuroiwa, T.; Ito, A. A Capacitive-Type Humidity Sensor Using Cross-Linked Poly(methyl methacrylate) Thin Films. *J. Electrochem. Soc.* **1991**, *138*, 1862−1865.
(39) Ho, D.; Sun, Q.; Kim, S.; Han, J.; Kim, D.; Cho, J. Stretchable and Multimodal All Graphene Electronic Skin. *Adv. Mater.* **2016**, *28*, 2601−2608.
(40) Viry, L.; Levi, A.; Totaro, M.; Mondini, A.; Mattoli, V.; Mazzolai, B.; Beccai, L. Flexible Three-Axial Force Sensor for Soft and Highly Sensitive Artificial Touch. *Adv. Mater.* **2014**, *26*, 2659−2664.
(41) Tung, Y.-C.; Shin, K. G. ForcePhone: Software Lets Smartphones Sense Touch Force. *IEEE Perv. Comp.* **2016**, *15*, 20−25.
(42) Wang, K.; Chang, Y.-H.; Chen, Y.; Zhang, C.; Wang, B. Designable Dual-Material Auxetic Metamaterials using Three-Dimensional Printing. *Mater. Eng.* **2015**, *67*, 159−164.
(43) Mousanezhad, D.; Babaee, S.; Ebrahimi, H.; Ghosh, R.; Hamouda, A. S.; Bertoldi, K.; Vaziri, A. Hierarchical Honeycomb Auxetic Metamaterials. *Sci. Rep.* **2016**, *5*, 18306.
(44) Someya, T.; Kato, Y.; Sekitani, T.; Iba, S.; Noguchi, Y.; Murase, Y.; Kawaguchi, H.; Sakurai, T. Conformable, Flexible, Large-Area Networks of Pressure and Thermal Sensors with Organic Transistor Active Matrixes. *Proc. Natl. Acad. Sci. U. S. A.* **2005**, *102*, 12321−12325.
(45) Takahashi, T.; Takei, K.; Gillies, A. G.; Fearing, R. S.; Javey, A. Carbon Nanotube Active-Matrix Backplanes for Conformal Electronics and Sensors. *Nano Lett.* **2011**, *11*, 5408−5413.
(46) Yeo, W.-H.; Kim, Y.-S.; Lee, J.; Ameen, A.; Shi, L.; Li, M.; Wang, S.; Ma, R.; Jin, S. H.; Kang, Z.; Huang, Y.; Rogers, J. A. Multifunctional Epidermal Electronics Printed Directly Onto the Skin. *Adv. Mater.* **2013**, *25*, 2773−2778.

DOI: 10.1021/acsnano.7b02474
ACS Nano 2017, 11, 7950−7957